Journal of Hazardous Materials 187 (2011) 164–170

Contents lists available at ScienceDirect

Journal of Hazardous Materials

journal homepage: www.elsevier.com/locate/jhazmat

Adsorption of food dyes acid blue 9 and food yellow 3 onto chitosan: Stirring rate effect in kinetics and mechanism

G.L. Dotto, L.A.A. Pinto*

Unit Operation Laboratory, School of Chemistry and Food, Federal University of Rio Grande – FURG, 475 Engenheiro Alfredo Huch Street, 96201-900 Rio Grande, RS, Brazil

ARTICLE INFO

Article history:
Received 22 July 2010
Received in revised form
22 November 2010
Accepted 4 January 2011
Available online 13 January 2011

Keywords:
Chitosan
Intraparticle diffusion
Film diffusion
Food dyes

ABSTRACT

Adsorption of food dyes acid blue 9 and food yellow 3 onto chitosan was studied. Stirring rate influence on kinetics and mechanism was verified. Infra-red analysis was carried out before and after adsorption in order to verify the adsorption nature. Adsorption experiments were carried out in batch systems with different stirring rates (15–400 rpm). Kinetic behavior was analyzed through the pseudo-first-order, pseudo-second-order and Elovich models. Adsorption mechanism was verified according to the film diffusion model and HSDM model. Pseudo-second-order and Elovich models were satisfactory in order to represent experimental data in all stirring rates. For both dyes, adsorption occurred by film and intraparticle diffusion, and the stirring rate increase caused a decrease in film diffusion resistance. Therefore, the film diffusivity increased the adsorption capacity and, consequently, intraparticle diffusivity increased. In all stirring rates, the rate-limiting step was film diffusion. Adsorption of acid blue 9 and food yellow 3 onto chitosan occurred by chemiosorption.

1. Introduction

Annually, the amount of dyes produced reaches about 10^5 tons [1], out of which 50% is lost in manufacturing and processing units [2]. Wastewater effluents from many industries such as textiles, rubber, food, paper and plastics, contain several kinds of dyes [3]. The release of these effluents causes coloration of surface waters and the colored effluent blocks the photosynthetic bacteria and aquatic plants from sunlight, interfering with the ecology of the receiving water [4]. An effective method for removal of dyes from wastewater is adsorption, due to its simplicity and high efficiency, as well as the availability of a wide range of adsorbents [5–7]. Chitosan is a cationic biopolymer used in order to remove dyes from effluents in adsorption systems, due to its high adsorption capacities and low-cost materials obtained from natural resources [8]. Most studies of dye adsorption onto chitosan are related to textile dyes [1,3,5,9,10], food dyes have rarely been investigated [11,12].

In food dye adsorption onto chitosan, kinetic and mechanism are important factors that control the process [8]. Kinetics control efficiency of the process [3] and explain how fast the reaction occurs and also leads to information on the factors affecting the reaction rate, and adsorption mechanism shows the interactions occurring at the adsorbent/adsorbate interface [8] in particular. In order to describe the adsorption kinetic process, adsorption reaction models (pseudo-first-order, pseudo-second order and Elovich equations) are applied [13]. These models are satisfactory in various cases, but, not always gives enough information to establish the adsorption mechanism [14], so, to elucidate a mechanism completely, adsorption diffusion models are used [13]. This way, a complete study to elucidate adsorbent/adsorbate interactions involves adsorption reaction models and adsorption diffusion models.

In general, the mechanism for dye removal by adsorption involves bulk diffusion, film diffusion, intraparticle diffusion and chemical reaction. In acid dye adsorption onto chitosan, bulk diffusion can be negligible [8] and chemical reaction is very fast [15], so, generally, the process is controlled by film diffusion or/and intraparticle diffusion. These mechanisms can be affected by various factors, including pH, ionic strength, dye concentration, dye chemistry, chitosan dosage and stirring rate. Stirring rate is an important parameter in adsorption phenomena, influencing the distribution of the solute in the bulk solution and the formation of the external boundary film [16]. A limited number of studies were carried out in relation to stirring rate effect on dye adsorption onto chitosan [17,18]. In addition, in these studies, stirring rate range changed from 100 to 200 rpm. Thus, an ample study of stirring rate range of food dye adsorption onto chitosan is desirable in order to verify how it affects adsorption behavior.

The aim of this study was to analyze stirring rate effect in the kinetic and mechanism of adsorption of acid blue 9 and food yellow 3 onto chitosan. Kinetic data were evaluated according to adsorption reaction models (pseudo-first-order, pseudo-second-order and Elovich equations) and mechanisms were evaluated

* Corresponding author. Tel.: +55 53 3233 8648; fax: +55 53 3233 8745.
E-mail address: dqmpinto@furg.br (L.A.A. Pinto).

0304-3894/$ – see front matter © 2011 Elsevier B.V. All rights reserved.
doi:10.1016/j.jhazmat.2011.01.016

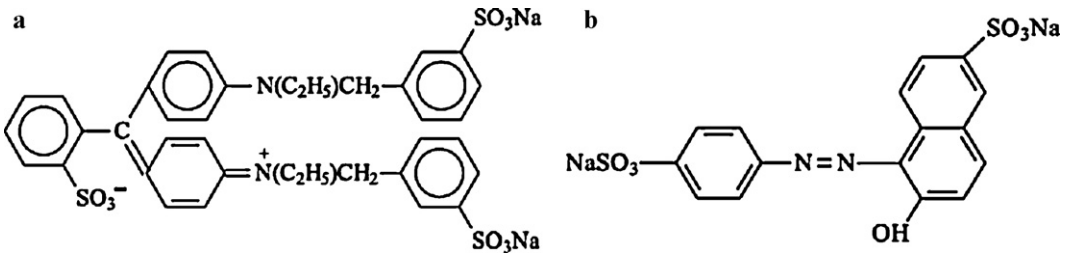

Fig. 1. Chemical structures of the dyes: (a) acid blue 9 and (b) food yellow 3.

according to HSDM model and film diffusion model. Infra-red analysis was carried out in order to verify adsorption nature.

2. Materials and methods

2.1. Adsorbate

Two food dyes were used in this study, the azo dye food yellow 3 (color index 15,985, molar mass 452.37 g mol^{-1}, purity 85%) and triarylmethane dye acid blue 9 (color index 42,090, molar mass 792.84 g mol^{-1}, purity 85%) (Plury Chemical Ltd., Brazil). Fig. 1 shows chemical structure of the dyes. All other utilized reagents were of analytical-reagent grade. Distilled water was used to prepare all solutions.

2.2. Adsorbent

The adsorbent used in this work was chitosan powder. Chitosan paste was obtained from shrimp wastes [19], dried [20] and characterized according to particle size (D) (Sauter definition), molar weight (Mw) (viscosimetric method) [21] and deacetylation degree (DD) (FT-IR analysis) [22]. Chitosan powder showed D = 70 μm, Mw = 150 kDa and DD = 86%.

2.3. Adsorption experiments

Chitosan samples (250 mg) were diluted in 0.8 L of distilled water and had their pH corrected (pH 3) with dissodic phosphate/citric acid 0.1 N. The pH 3 was chosen because according to Crini and Badot [8] an optimal range for dye adsorption onto chitosan is from 3 to 6, and below this range, usually a large excess of competitor anions limits adsorption efficiency. In addition, preliminary tests showed that the pH decrease from 6 to 3 caused an increase in adsorption capacity. Preliminary tests were carried out in order to verify the chitosan stability in relation to pH. These tests showed that in the range of experiments, chitosan maintain its total integrity and gel structure was not formed. This manner, in the range of experiments, adsorption dyes occurred only in chitosan soluble powder.

Solutions were agitated for 30 min so that pH reached the equilibrium, this being measured (Mars, MB10, Brazil) before and after the adsorption process. 50 mL of solution were added with 2 g L^{-1} of dye to each solution of chitosan, and completed to 1 L with distilled water, so that the initial concentration of dye was 100 mg L^{-1} in all solutions [3].

The experiments were carried out in a jar test (Miller, JP101, Brazil) under room temperature (25 ± 1 °C). The stirring rates used were 15, 50, 100, 200 and 400 rpm. This range was based in preliminary tests (the tests showed that the adsorption capacity is not influenced in stirring rate above 400 rpm, and reaching a maximum value in this condition). Aliquots were removed in intervals of preset times (2–120 min). To obtain the equilibrium adsorption capacity (q_e), aliquots were removed in 24, 36 and 48 h. Dye concentration was determined by spectrophotometer (Quimis, Q108 DRM, Brazil) at 408 and 480 nm for acid blue 9 and food yellow 3, respectively. Adsorption capacity at time t (q_t) was determined by Eq. (1):

$$q_t = \frac{V(C_0 - C_t)}{m} \quad (1)$$

where V is the volume of solution (L), m is the chitosan amount (g), C_0 and C_t are the initial dye concentration in liquid phase and at the concentration after time t (mg L^{-1}).

2.4. Kinetic models

In order to analyze adsorption kinetic behavior of acid blue 9 and food yellow 3 onto chitosan, adsorption reaction models were used [5,9,10,23,24].

The kinetic models of pseudo-first order and pseudo-second order assume that adsorption is a pseudo-chemical reaction, and the adsorption rate can be determined, respectively, for equations of pseudo-first (Eq. (2)) and pseudo-second order (Eq. (3)) [25]:

$$q_t = q_1(1 - \exp(-k_1 t)) \quad (2)$$

$$q_t = \frac{t}{(1/k_2 q_2^2) + (t/q_2)} \quad (3)$$

where q_t is the adsorbate amount adsorbed at time t (mg g^{-1}), k_1 and k_2 are the rate constants of pseudo-first and pseudo-second-order models, respectively, in (min^{-1}) and (g mg^{-1} min^{-1}), q_1 and q_2 are the theoretical values for the adsorption capacity (mg g^{-1}) and t is the time (min).

When the adsorption processes occurs through chemiosorption in solid surface, and the adsorption velocity decreases with time due to covering of the superficial layer, the Elovich model is most used. The Elovich kinetic model is described according to Eq. (4) [26]:

$$q_t = \frac{1}{a}\ln(1 + abt) \quad (4)$$

where "a" is the initial velocity due to dq/dt with q_t = 0 (mg g^{-1} min^{-1}) and "b" is the desorption constant of the Elovich model (g mg^{-1}).

2.5. Mechanism models

To indentify the different mechanisms that occur in the process, the adsorption capacity as a function of the square root of time was plotted [27]. In order to estimate film diffusion and intraparticle diffusion values, experimental data were fitted with film diffusion model and HSDM model.

Crank [28], based in Fick law showed a model for diffusion in the boundary layer between adsorbent and the solution (film diffusion), this model is shown in Eq. (5):

$$\frac{q_t}{q_e} = 6\left(\frac{D_f}{\pi R_p^2}\right)^{0.5} t^{0.5} \quad (5)$$

where D_f is the film diffusivity ($m^2\ min^{-1}$) and R_p is the average ray of the adsorbent particle (m) and q_e is the equilibrium adsorption capacity ($mg\ g^{-1}$).

When mass transfer resistance is internal, intraparticle diffusion controls the process. In this case considering diffusivity constant, particle amorphous, homogeneous and spherical, and the external resistance being negligible, the adsorption process can be represented by HSDM model, Eq. (6) [13,29]:

$$\frac{\partial q}{\partial t} = D_P\left(\frac{\partial^2 q}{\partial r^2} + \frac{2}{r}\frac{\partial q}{\partial r}\right) \quad (6)$$

Using appropriate boundary and initial conditions, and considering a linear isotherm between initial and final concentration, for finite volume process, Crank [28], developed a solution that can be approximated to the first term of series when the Fourier number is higher than 0.2, Eq. (7):

$$\frac{q}{q_e} = 1 - \left[\frac{6\alpha(\alpha+1)\exp(-q_n^2 D_P t/R_P^2)}{9+9\alpha+q_n^2\alpha^2}\right] \quad (7)$$

where D_P is the intraparticle diffusivity ($m^2\ min^{-1}$), α is the effective volume ratio, expressed as a function of the equilibrium partition coefficient (solid/liquid concentration ratio) and is obtained by the ratio ($C_e/C_0 - C_e$) and q_n represents the non-zero solutions of Eq. (8):

$$\tan q_n = \frac{3q_n}{3+\alpha q_n^2} \quad (8)$$

2.6. Regression analysis

The coefficients of the kinetic and mechanisms equations were determined by nonlinear regression, using Statistic 6.0 software (Statsoft, USA), verifying its fit through correlation coefficients (R^2) and average relative error (ARE) (Eq. (9)):

$$ARE = \frac{100}{n}\sum_{1}^{n}\frac{q_{t,exp} - q_{t,pre}}{q_{t,pre}} \quad (9)$$

where $q_{t,exp}$ and $q_{t,pre}$ are the experimental values of adsorption capacity in time "t" and obtained from kinetics and mechanism models.

2.7. Adsorption nature

Adsorption process nature was verified through infra-red analysis (FT-IR analysis). Chitosan samples were removed before and after the adsorption process, and were dried (105 °C) until constant weight. Later, samples were macerated and submitted to the spectroscopic determination in the region of the infra-red ray (Prestige 21, the 210045, Japan), using the technique of diffuse reflectance in potassium bromide [30].

3. Results and discussion

3.1. Stirring rate effect in adsorption kinetic

In order to analyze the stirring rate effect in adsorption kinetic behavior, adsorption capacity values were plotted as a function of time. Figs. 2 and 3 show, adsorption capacity as a function of time for acid blue 9 and food yellow 3, respectively, in all stirring rates studied.

In Figs. 2 and 3, the kinetic curves showed that in all stirring rates for both dyes, adsorption was fast, reaching about 80% of saturation in 30 min. Later, adsorption rate decreased considerably. Fast kinetic is characteristic in dye–chitosan systems and is desirable in wastewater treatment because it leads high adsorption capacities

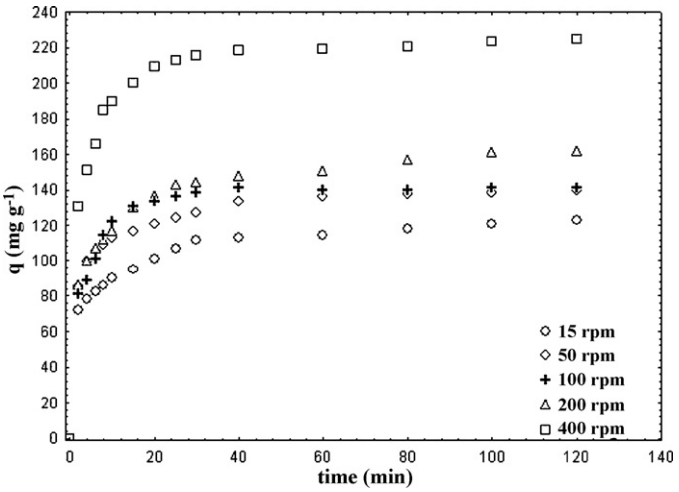

Fig. 2. Acid blue 9 adsorption capacity with different stirring rate.

in short times. Kyzas and Lazaridis [31] obtained similar results in their work; they used chitosan and chitosan derivatives to remove remazol yellow and basic yellow 37 by adsorption, and obtained up to 95% of dye removal percentage in 50 min.

In Fig. 2 it can be observed that the increase in stirring rate from 15 to 400 rpm leads to a large increase in acid blue 9 adsorption capacity, from 110 $mg\ g^{-1}$ to 220 $mg\ g^{-1}$. In the same way, for the food yellow 3 (Fig. 3), an increase in stirring rate from 15 to 400 rpm increased adsorption capacity from 220 $mg\ g^{-1}$ to 350 $mg\ g^{-1}$. According to Crini and Badot [8] this behavior can be explained because an increase in the degree of agitation increased the mobility of the system. In addition, agitation increase by increase of stirrer speed lowers the external mass transfer effect. Similar behavior was found by Uzun and Guzel [17] in adsorption of orange II and crystal violet onto chitosan. On the other hand, the stirring rate increase from 50 to 100 rpm, for acid blue 9, and from 50 to 200 rpm for food yellow 3 caused a little increase in adsorption capacity. According to Ruthven [29], this occurs because, the stirring rates from 50 to 200 are in the average range of agitations rates, and generally in this range occurs little alterations in adsorption behavior.

In Figs. 2 and 3, it can be observed that food yellow 3 adsorption capacity was higher than acid blue 9 adsorption capacity. This occurs because acid blue 9 molar weight is higher than food yellow 3 molar weight, and acid blue 9 is more ramified, so, causing

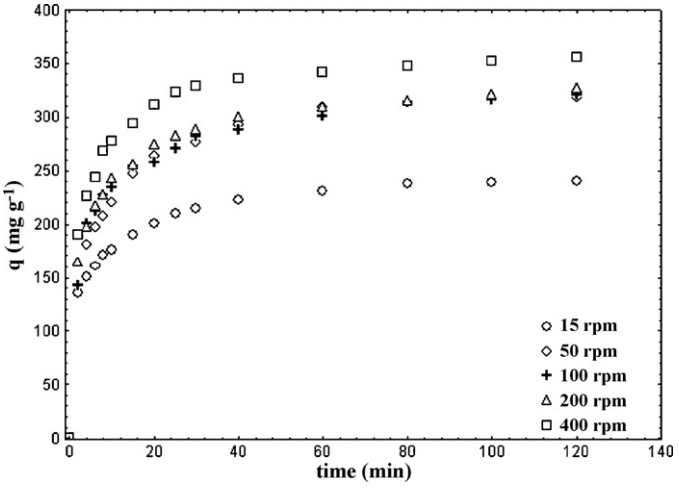

Fig. 3. Food yellow 3 adsorption capacity with different stirring rate.

difficulty in dye diffusion. This behavior was observed by Cestari et al. [32] in adsorption of anionic dyes on chitosan beads. In this study they show that dimensions of the dye organic chains, amount and positioning of the sulfonate groups of the dyes influence dye adsorption by chitosan.

Pseudo-first-order, pseudo-second-order and Elovich models were used to fit the experimental data and thus elucidate the adsorption kinetics. Parameters of pseudo-first-order, pseudo-second-order and Elovich models, coefficients of determination (R^2) and average relative error (ARE) are shown in Table 1.

In Table 1 it can be observed that in all stirring rates for both dyes, pseudo-first-order model did not show a good fit with experimental data ($R^2 < 0.95$ and ARE > 5%). Pseudo-first-order model assumes that adsorption occurs due to a concentration difference between adsorbate surface and solution. This occurs only in adsorption and begins when external mass transfer coefficient controls the process [8]. This shows that adsorption of acid blue 9 and food yellow 3 onto chitosan was not only controlled by external mass transfer coefficient.

On the other hand, pseudo-second-order and Elovich models showed a good fit with experimental data ($R^2 > 0.95$ and ARE < 5%) (Table 1). Pseudo-second-order model had the same equation for internal and external mass transfer mechanism [25], and Elovich model is used when chemiosorption occurs and adsorption rate decreases with time due to saturation of adsorption sites in the surface [26]. In this manner, a good fit with pseudo-second-order and Elovich model suggest that adsorption of acid blue 9 and food yellow 3 onto chitosan occurs by internal and external mass transfer mechanisms, the adsorption process being by chemical nature. Similar behavior was obtained by Singh et al. [10] in dyes adsorption onto grafted chitosan. In their work pseudo-second-order model was satisfactory to represent experimental data, admitting the chemical nature of dye adsorption onto grafted chitosan.

Kinetic analysis showed that adsorption of acid blue 9 and food yellow 3 onto chitosan had a fast kinetic, and the stirring rate increase caused an increase in adsorption capacity. In all stirring rates used, the process occurs through external and internal mass transfer mechanism, adsorption being by chemical nature.

3.2. Stirring rate effect in adsorption mechanism

To identify the mass transfer steps in different stirring rates adsorption capacities as a function of square root of time were plotted [27]. According to Weber and Morris [27], the plot q_t versus $t^{1/2}$ shows multi linearity, and each portion represents a distinct mass transfer mechanism. The first portion is the external mass transfer (film diffusion) or instantaneous adsorption step. The second portion is the gradual adsorption step where the intra-particle diffusion can be rate controlling. The third portion is the final equilibrium step where the intra-particle diffusion starts to slow down due to the extremely low solute concentration in the solution [33]. In addition, if the regression passes through the origin, then intra-particle diffusion is the sole rate-limiting step. Figs. 4 and 5 show, respectively, the Weber and Morris plots for acid blue 9 and food yellow 3 in all stirring rates used.

From Figs. 4 and 5, multi linearity with two distinct phases can be observed. The initial portion relates to the boundary layer diffusion (film diffusion). The second portion describes the gradual adsorption step, where intraparticle diffusion control is rate limiting. This shows that film diffusion and intra-particle diffusion were simultaneously operating during the adsorption process of acid blue 9 and food yellow 3 onto chitosan. Stirring rate increase caused a decrease in film diffusion effect, and consequently, increase in intraparticle diffusion effect (Figs. 4 and 5). For both dyes, using 15 rpm, the process occurs by film diffusion until 40 min, but, when stirring rate was increased to 400 rpm the process occurs by film

Table 1
Experimental data fit with adsorption reaction models.

Dye	Stirring rate (rpm)	Pseudo-first-order				Pseudo-second-order				Elovich			
		q_1 (mg g^{-1})	k_1 (min^{-1})	R^2	ARE (%)	q_2 (mg g^{-1})	k_2 (g mg^{-1} min^{-1})	R^2	ARE (%)	a (g mg^{-1})	b (mg g^{-1} min^{-1})	R^2	ARE (%)
Acid blue 9	15	109.6	0.29	0.87	8.4	117.6	0.018	0.96	4.6	0.076	956.8	0.99	1.8
	50	127.7	0.39	0.92	6.3	136.0	0.011	0.98	3.2	0.074	1234.2	0.99	1.3
	100	137.1	0.25	0.90	7.6	145.4	0.016	0.97	3.8	0.066	2790.0	0.99	1.8
	200	146.2	0.27	0.91	5.6	157.2	0.014	0.99	2.6	0.052	6394.0	0.96	4.3
	400	213.2	0.32	0.92	5.6	226.0	0.008	0.99	1.5	0.045	7869.6	0.97	4.0
Food yellow 3	15	217.8	0.27	0.89	8.2	234.1	0.009	0.97	4.3	0.036	627.7	0.99	1.2
	50	292.2	0.19	0.91	8.3	318.2	0.011	0.98	4.1	0.025	1210.4	0.99	2.0
	100	288.2	0.24	0.92	7.2	312.4	0.008	0.98	3.2	0.025	1593.3	0.99	2.4
	200	295.2	0.24	0.91	7.3	318.3	0.008	0.98	3.2	0.024	1777.0	0.99	2.2
	400	329.3	0.27	0.93	6.2	352.6	0.006	0.99	2.3	0.022	3294.3	0.99	2.8

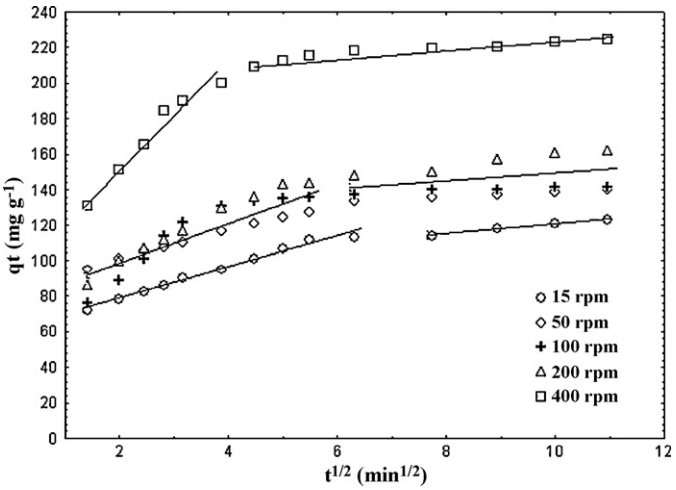

Fig. 4. Stirring rate effect in adsorption mechanism of acid blue 9.

diffusion until 20 min. This behavior can be explained because stirring rate increase causes a decrease in film thickness and consequently decreases boundary layer diffusion resistance.

In order to estimate film diffusivity and intraparticle diffusivity, experimental data relative to first portion of Weber–Morris plot was fitted with film diffusion model (Eq. (5)), and experimental data of second portion were fitted with HSDM solution (Eq. (7)). Table 2 shows film and intraparticle diffusivity values, correlation coefficients (R^2) and average relative error (ARE).

In Table 2 it can be observed that film diffusion model showed a good fit with experimental data relative to first portion of Weber–Morris plot, and HSDM model showed a good fit with experimental data of second portion ($R^2 > 0.95$ and $E < 5\%$), justifying adsorption mechanisms. Thus, film and intraparticle diffusivities were estimated. For both dyes, the increase in stirring rate caused an increase in film diffusivity. According to Suzuki [34], in adsorption systems, the stirring rate increase causes an increase in film diffusivity. This increase in film diffusivity facilitates food dye diffusion, increasing adsorption capacity. The intraparticle diffusivity increase was a consequence only of adsorption capacity increase. Intraparticle diffusivity value largely depends on the surface properties of adsorbents and adsorption capacity [29], being independent of stirring rate.

Comparing film diffusivities with intraparticle diffusivities (Table 2) it can be observed that in all stirring rates, the process

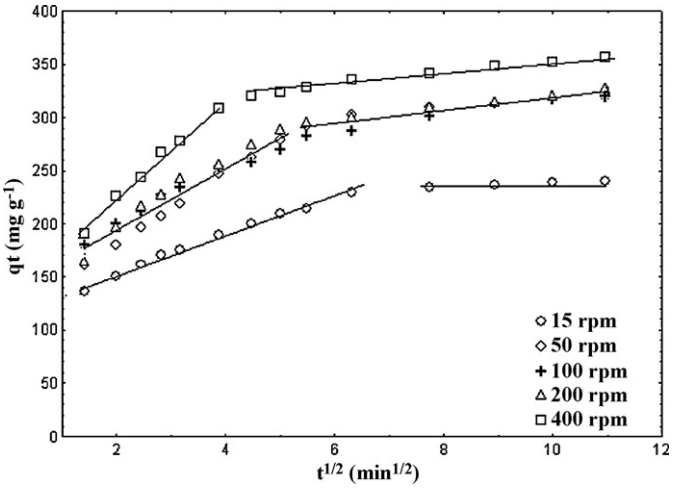

Fig. 5. Stirring rate effect in adsorption mechanism of food yellow 3.

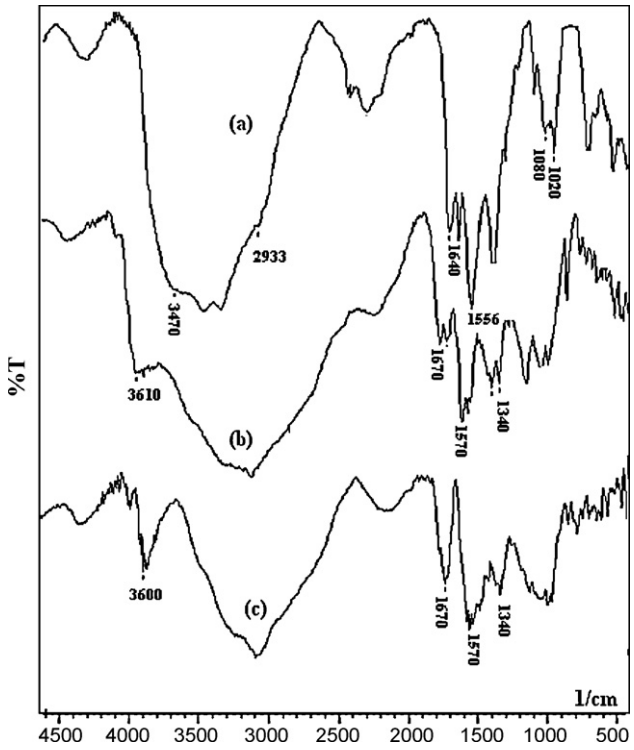

Fig. 6. FT-IR analysis: (a) chitosan, (b) chitosan adsorbed with acid blue 9, and (c) chitosan adsorbed with food yellow 3.

was controlled by film diffusion ($D_p > D_f$). This suggests that after dye molecules cross the boundary layer, they are rapidly adsorbed into chitosan adsorption sites. Similar behavior was observed by Noroozi et al. [33] in cationic dye adsorption onto silkworm pupa. In their work, assumed that film diffusion and intraparticle diffusion were simultaneously operating during the process, but, film diffusion was the rate-limiting process.

The mechanism analysis showed that food dyes adsorption onto chitosan occurred by film diffusion and intraparticle diffusion, and stirring rate increase caused a decrease in film diffusion effect. Stirring rate increase caused an increase in film diffusivity, and adsorption capacity increase caused an increase in intraparticle diffusivity. In all stirring rates adsorption process was controlled by film diffusion.

3.3. Adsorption nature

Fig. 6 shows FT-IR analysis of (a) chitosan, (b) chitosan adsorbed with acid blue 9, and (c) chitosan adsorbed with food yellow 3.

In Fig. 6(a), peaks in 1556 cm^{-1}($-NH_2$), 1640 cm^{-1} (amide I band), 1020 cm^{-1} and 1080 cm^{-1} (C–N), 2933 cm^{-1} (N–H) can be observed. These peaks are involved in the functional group of amine on chitosan polymer. In addition, in 3470 cm^{-1} the hydroxyl groups linked in the chitosan structure can be observed. After the adsorption process it can be observed in Fig. 6(b) and (c) that at peaks 1556 cm^{-1} and 1640 cm^{-1} were shifted to peaks 1570 cm^{-1} and 1670 cm^{-1}, respectively, in addition, a new peak appeared in 1340 cm^{-1}. According to Sakkayawong et al. [30] the peak in this area is a sulfonated group in the ring of the dye. These peaks changes and a new peak confirm the attachment of dyes sulfonate groups on the chitosan amino groups. In addition, peak 3470 cm^{-1} (Fig. 6(a)) changed to 3600 and 3610 cm^{-1} (Fig. 6(b) and (c)), showing hydroxyl groups protonation and its attachment on sulfonated groups of the dyes. Interactions between chitosan amino groups and sulfonated groups of the dyes were related by other

Table 2
Film diffusion and intraparticle diffusivity models.

Dye	Stirring rate (rpm)	Film diffusion model			HSDM model		
		$D_f \times 10^{14}$ ($m^2\ min^{-1}$)	R^2	ARE (%)	$D_p \times 10^{14}$ ($m^2\ min^{-1}$)	R^2	ARE (%)
Acid blue 9	15	4.7	0.99	0.4	38	0.98	0.3
	50	16.6	0.99	1.2	109	0.97	0.2
	100	18.0	0.99	1.7	113	0.97	0.4
	200	53.8	0.99	1.4	275	0.97	1.0
	400	63.3	0.96	2.2	521	0.97	0.8
Food yellow 3	15	24.6	0.99	1.5	48	0.97	0.1
	50	72.8	0.99	0.6	733	0.97	0.2
	100	75.7	0.97	1.8	740	0.97	0.7
	200	76.5	0.96	2.7	750	0.98	0.3
	400	158.9	0.99	1.2	1800	0.98	0.3

works [8,12], even as interactions of chitosan hydroxyl groups and sulfonated groups of the dyes [15]. Thus it can be affirmed that adsorption of acid blue 9 and food yellow 3 onto chitosan occurred by chemiosorption, and chitosan amino and hydroxyl groups were responsible for dyes adsorption.

4. Conclusion

In this research the stirring rate effect on kinetic and mechanism of adsorption of acid blue 9 and food yellow 3 onto chitosan was studied. FT-IR analysis was carried out in order to verify adsorption nature. A stirring rate increase from 15 to 400 rpm doubled the acid blue 9 adsorption capacity and increased in 60% the food yellow 3 adsorption capacity. In all stirring rates, pseudo-second-order and Elovich models were satisfactory in order to represent experimental data ($R^2 > 0.95$ and ARE < 5%), suggesting that the adsorption process was chemical and occurred through internal and external mass transfer mechanisms.

In adsorption of acid blue 9 and food yellow 3 onto chitosan, the mechanism study showed that film diffusion and intraparticle diffusion occurred simultaneously and stirring rate increase caused a decrease in film diffusion resistance. The good fit of film diffusion and HSDM models ($R^2 > 0.95$ and ARE < 5%) justified adsorption mechanisms. Stirring rate increase caused an increase in film diffusivity and adsorption capacity increase caused an increase in intraparticle diffusivity. Although film diffusion and intraparticle diffusion occurred simultaneously, film diffusion was the rate limiting step in adsorption process.

FT-IR analysis showed that adsorption of acid blue 9 and food yellow 3 onto chitosan occurred by chemiosorption between amino and hydroxyl groups of chitosan and sulfonated groups of the dyes.

Acknowledgements

The authors would like to thank CAPES (Brazilian Agency for Improvement of Graduate Personnel) and CNPq (National Council of Science and Technological Development) for the financial support.

References

[1] K.Z. Elwakeel, Removal of reactive black 5 from aqueous solutions using magnetic chitosan resins, J. Hazard. Mater. 167 (2009) 383–392.
[2] R. Patel, S. Suresh, Kinetic and equilibrium studies on the biosorption of reactive black 5 dye by *Aspergillus foetidus*, Bioresour. Technol. 99 (2008) 51–58.
[3] G. Annadurai, L.Y. Ling, J.F. Lee, Adsorption of reactive dye from an aqueous solution by chitosan: isotherm, kinetic and thermodynamic analysis, J. Hazard. Mater. 152 (2008) 337–346.
[4] W.H. Cheung, Y.S. Szeto, G. McKay, Enhancing the adsorption capacities of acid dyes by chitosan nano particles, Bioresour. Technol. 100 (2009) 1143–1148.
[5] L. Lian, L. Guo, C. Guo, Adsorption of Congo red from aqueous solutions onto Ca bentonite, J. Hazard. Mater. 161 (2009) 126–131.
[6] M. Turabik, Adsorption of basic dyes from single and binary component systems onto bentonite: simultaneous analysis of basic red 46 and basic yellow 28 by first order derivative spectrophotometric analysis method, J. Hazard. Mater. 158 (2008) 52–64.
[7] M. Asadullaha, M. Asaduzzamana, M.S. Kabira, M.G. Mostofa, T. Miyazawac, Chemical and structural evaluation of activated carbon prepared from jute sticks for brilliant green dye removal from aqueous solution, J. Hazard. Mater. 174 (2010) 437–443.
[8] G. Crini, P.M. Badot, Application of chitosan, a natural aminopolysaccharide, for dye removal from aqueous solutions by adsorption processes using batch studies: a review of recent literature, Prog. Polym. Sci. 33 (2008) 399–447.
[9] A.H. Chen, S.M. Chen, Biosorption of azo dyes from aqueous solution by glutaraldehyde-crosslinked chitosans, J. Hazard. Mater. 172 (2009) 1111–1121.
[10] V. Singh, A.K. Sharma, D.N. Tripathi, R. Sanghi, Poly (methylmethacrylate) grafted chitosan: an efficient adsorbent for anionic azo dyes, J. Hazard. Mater. 161 (2009) 955–966.
[11] A.R. Cestari, E.F.S. Vieira, A.M.G. Tavares, R.E. Bruns, The removal of the indigo carmine dye from aqueous solutions using cross-linked chitosan-evaluation of adsorption thermodynamics using a full factorial design, J. Hazard. Mater. 153 (2008) 566–574.
[12] J.S. Piccin, M.L.G. Vieira, J. Gonçalves, G.L. Dotto, L.A.A. Pinto, Adsorption of FD&C Red No. 40 by chitosan: isotherms analysis, J. Food Eng. 95 (2009) 16–20.
[13] H. Qiu, L.L. Pan, Q.J. Zhang, W. Zhang, Q. Zhang, Critical review in adsorption kinetic models, J. Zhejiang Univ. Sci. A 10 (2009) 716–724.
[14] N.K. Lazaridis, T.D. Karapantsios, D. Georgantas, Kinetic analysis for the removal of a reactive dye from aqueous solution onto hydrotalcite by adsorption, Water Res. 37 (2003) 3023–3033.
[15] S. Stefancich, F. Delben, R.A.A. Muzzarelli, Interactions of soluble chitosans with dyes in water. I. Optical evidence, Carbohydr. Polym. 24 (1994) 17–23.
[16] G. Crini, Recent developments in polysaccharide-based materials used as adsorbents in wastewater treatment, Prog. Polym. Sci. 30 (2005) 38–70.
[17] I. Uzun, F. Guzel, Kinetics and thermodynamics of the adsorption of some dyestuffs and p-nitrophenol by chitosan and MCM-chitosan from aqueous solution, J. Colloid Interface Sci. 274 (2004) 398–412.
[18] I. Uzun, F. Guzel, Rate studies on the adsorption of some dyestuffs and p-nitrophenol by chitosan and monocarboxymethylated (mcm) chitosan from aqueous solution, J. Hazard. Mater. 118 (2005) 141–154.
[19] R.F. Weska, J.M. Moura, L.M. Batista, J. Rizzi, L.A.A. Pinto, Optimization of deacetylation in the production of chitosan from shrimp wastes: use of response surface methodology, J. Food Eng. 80 (2007) 749–753.
[20] C.Y. Halal, J. Moura, L.A.A. Pinto, Evaluation of molecular weight of chitosan in thin-layer and spouted bed drying, J. Food Proc. Eng. Proof (2010) 1–15.
[21] H. Zhang, S.H. Neau, In vitro degradation of chitosan by a commercial enzyme preparation: effect of molecular weight and degree of deacetylation, Biomaterials 22 (2001) 1653–1658.
[22] M.F. Cervera, J. Heinamaki, M. Rasanem, S.L. Maunu, M. Karjalainen, O.M.N. Acosta, A.I. Colarte, J. Yliruusi, Solid state characterization of chitosan derived from lobster chitin, Carbohydr. Polym. 58 (2004) 401–408.
[23] B.H. Hameed, D.K. Mahmoud, A.L. Ahmad, Sorption equilibrium and kinetics of basic dye from aqueous solution using banana stalk waste, J. Hazard. Mater. 158 (2008) 499–506.
[24] S. Liang, X. Guo, N. Feng, Q. Tian, Isotherms, kinetics and thermodynamic studies of adsorption of Cu^{2+} from aqueous solutions by Mg^{2+}/K^{+} type orange peel adsorbents, J. Hazard. Mater. 174 (2010) 756–762.
[25] G. Skodras, I.R. Diamantopoulou, G. Pantoleontos, G.P. Sakellaropoulos, Kinetic studies of elemental mercury adsorption in activated carbon fixed bed reactor, J. Hazard. Mater. 158 (2008) 1–13.
[26] F.C. Wu, R.L. Tseng, R.S. Juang, Characteristics of Elovich equation used for the analysis of adsorption kinetics in dye chitosan systems, Chem. Eng. J. 150 (2009) 366–373.
[27] W.J. Weber, J.C. Morris, Kinetics of adsorption of carbon from solutions, J. Sanit. Eng. Div. Am. Soc. Civ. Eng. 89 (1963) 31–63.
[28] J. Crank, The Mathematics of Diffusion, second ed., Clarendon Press, Oxford, 1975.
[29] D.M. Ruthven, Principles of Adsorption and Adsorption Processes, John Wiley & Sons, New York, 1984.

[30] N. Sakkayawong, P. Thiravetyan, W. Nakbanpote, Adsorption mechanism of synthetic reactive dye wastewater by chitosan, J. Colloid Interface Sci. 286 (2005) 36–42.
[31] G. Kyzas, N.K. Lazaridis, Reactive and basic dyes removal by sorption onto chitosan derivatives, J. Colloid Interface Sci. 331 (2009) 32–39.
[32] A.R. Cestari, E.F.S. Vieira, A.G.P. Santos, J.A. Mota, V.P. Almeida, Adsorption of anionic dyes on chitosan beads. 1. The influence of the chemical structures of dyes and temperature on the adsorption kinetics, J. Colloid Interface Sci. 280 (2004) 380–386.
[33] B. Noroozi, G.A. Sorial, H. Bahrami, M. Arami, Equilibrium and kinetic adsorption study of a cationic dye by a natural adsorbent-silkworm pupa, J. Hazard. Mater. 39 (2007) 167–174.
[34] M. Suzuki, Adsorption Engineering, Kodansha, Tokyo, 1990.